XIV International Conference on Topics in Astroparticle and Underground Physics (TAUP 2015) IOP Publishing
Journal of Physics: Conference Series **718** (2016) 042027 doi:10.1088/1742-6596/718/4/042027

Predicting the capture rate in the Sun from a direct detection signal independently of the astrophysics

Juan Herrero-Garcia
Department of Theoretical Physics, Royal Institute of Stockholm (KTH)
E-mail: juhg@kth.se

Abstract. The goal of the works on which this talk is based is to relate a direct detection signal with neutrino limits from the Sun independently of the astrophysics. In order to achieve this we derive a halo-independent lower bound on the dark matter capture rate in the Sun from a direct detection signal, with which one can set upper limits on the branching ratios into different channels from the absence of a high-energy neutrino flux in neutrino observatories. We also extend this bound to the case of inelastic scattering, both endothermic and exothermic. From two inelastic signals we show how the dark matter mass, the mass difference of the states and the couplings to neutrons and protons can be obtained. Furthermore, one can also pin down the exothermic/endothermic nature of the scattering, and therefore a precise lower bound on the solar capture rate is predicted. We also discuss isospin violation and uncertainties due to form factors.

1. Motivation: a new halo-independent framework

It is well-known that dark matter (DM) direct detection (DD) signals are very sensitive to the astrophysical uncertainties of the halo, which makes their compatibility with other results astrophysics-dependent. This talk is devoted to a new halo-independent (HI) framework to compare DD signals with upper limits from neutrino telescopes [1, 2].

Let us first review the basic expressions for DM DD and the well-known HI framework used for comparing among DD signals. For SI interactions, the DM event rate in underground detectors can be written as [3]

$$\mathcal{R}(E_R,t) = A_{\rm eff}^2 F_A^2(E_R)\tilde{\eta}(v_m,t), \quad \text{with} \quad \tilde{\eta}(v_m,t) \equiv \mathcal{C}\int_{v_m}^{\infty} dv\, v\, \tilde{f}_{\rm det}(v,t)\,, \tag{1}$$

where $f_{\rm det}(v)$ is the (unknown) velocity distribution in the detector rest-frame, $F_A(E_R)$ is a nuclear form factor, $A_{\rm eff}^2 = (Z+\kappa\,(A-Z))^2$ with $\kappa = f_n/f_p$ and

$$\tilde{f}_{\rm det}(v) \equiv \int d\Omega f_{\rm det}(v,\Omega), \qquad \mathcal{C} \equiv \frac{\rho_\chi \sigma_{\rm SI}}{2 m_\chi \mu_{\chi p}^2}, \qquad v_m = \left| \sqrt{\frac{m_A E_R}{2\mu_{\chi A}^2}} + \frac{\delta}{\sqrt{2\, m_A\, E_R}} \right|. \tag{2}$$

The mass-splitting parameter δ appears in inelastic interactions [4], given by $\delta \equiv m_{\chi^*} - m_\chi$, and thus it is positive (negative) for endothermic (exothermic [5]) interactions. For $\delta = 0$ elastic interactions are recovered. $\sigma_{\rm SI}$ is the total DM–proton scattering cross section at zero momentum transfer, $\mu_{\chi p}$ is the DM–proton reduced mass and ρ_χ is the local DM mass density.

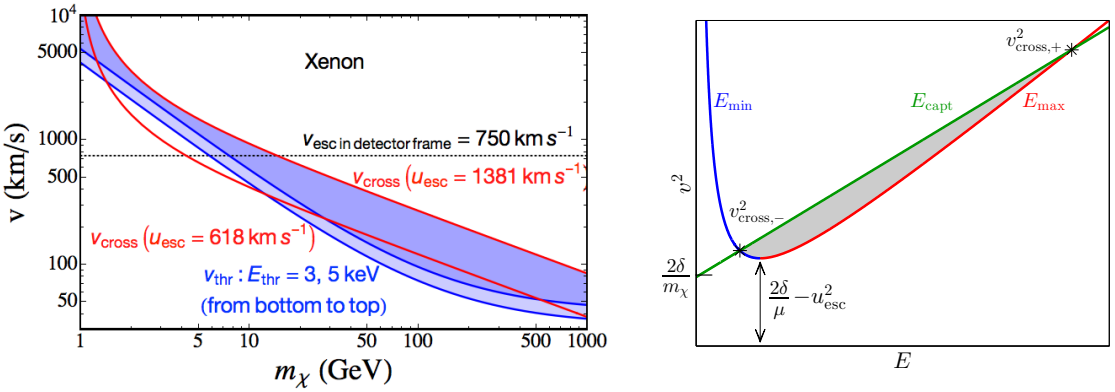

Figure 1. Left) $v_{\rm thr}$ (blue) probed in a Xe DD experiment versus m_χ, for $E_{\rm thr} = 3, 5$ keV. The maximum velocity for DM capture on hydrogen, $v^p_{\rm cross}$, is shown in red for $u_{\rm esc} = 1381\,{\rm km\,s^{-1}}$ (centre of the Sun) and $v_{\rm esc} = 618\,{\rm km\,s^{-1}}$ (surface). The shaded area shows the largest possible overlap region (for the centre of the Sun). The horizontal black line indicates approximately the galactic escape velocity in the detector rest frame. Right) The shaded area represents the horizontal integration needed for the capture rate in the case of inelastic scattering, see ref. [2] for details.

For fixed DM mass m_χ, one can translate recoil energies E_R into velocities v_m via eq. (2) and compare the halo integrals $\tilde{\eta}(v_m, t)$ of the different experiments, which have to be the same [6, 7]. This is the basis of the HI framework developed to compare among DD signals and limits, extended also to annual modulation signals [8, 9] in refs. [10, 11], and to inelastic scattering [12]. Recently in refs. [13, 14] a new HI framework was devised in order to compare a DD signal with limits from the LHC, the relic abundance and indirect detection.

As we will use it in the following section, let us remark that if a positive signal and an spectrum is detected in a DD experiment one can extract $\mathcal{C} \cdot \tilde{f}_{\rm det}(v)$ from the data using the following expression:

$$\mathcal{C}\tilde{f}_{\rm det}(v) = -\frac{1}{v}\frac{d\tilde{\eta}(v)}{dv} = -\frac{1}{vA^2}\frac{d}{dv}\left(\frac{\mathcal{R}(E_R)}{F_A^2(E_R)}\right), \tag{3}$$

where E_R is considered as a function of $v = v_m$ according to eq. (2), depending on the DM mass, and we have defined for constant rates $\overline{\eta}(v_m) \equiv \int_{v_m}^{\infty} dv\, v\, \tilde{f}_{\rm det}(v)$, in a similar way as in eq. (1).

2. A halo-independent lower bound on the capture rate

The capture rate of DM in the Sun is determined by the scattering cross section of the DM particles on nuclei, the same process which provides the DD signals. However the DD signal and the DM capture in the Sun depend on different regions of the DM velocity distribution. While DD experiments are sensitive to DM particles with velocity larger than a certain minimal velocity $v_m(E_{\rm th}) \equiv v_{\rm thr}$, see eq. (2), the DM capture in the Sun is sensitive to values below a certain maximum velocity $v^A_{\rm cross}(r)$, above which capture is kinematically forbidden [15, 16, 17]. Therefore DD signals and capture rates can be related in the region $v_{\rm thr} < v < v^A_{\rm cross}(r)$. This is shown in fig. 1.

Using that $f(v)_{\rm sun} \simeq f_{\rm det}(v) \equiv f(v)$, and that both $f(v)$ and ρ_χ are constant on equilibration times, we can derive a lower bound on the capture rate (see ref. [1] for more details):

$$C_{\rm Sun} = 4\pi\,\mathcal{C} \sum_A A^2_{\rm eff} \int_0^{R_{\rm S}} dr r^2 \rho_A(r) \int_0^{v^A_{\rm cross}} dv \tilde{f}(v)\, v\, \mathcal{F}_A(v, r)$$

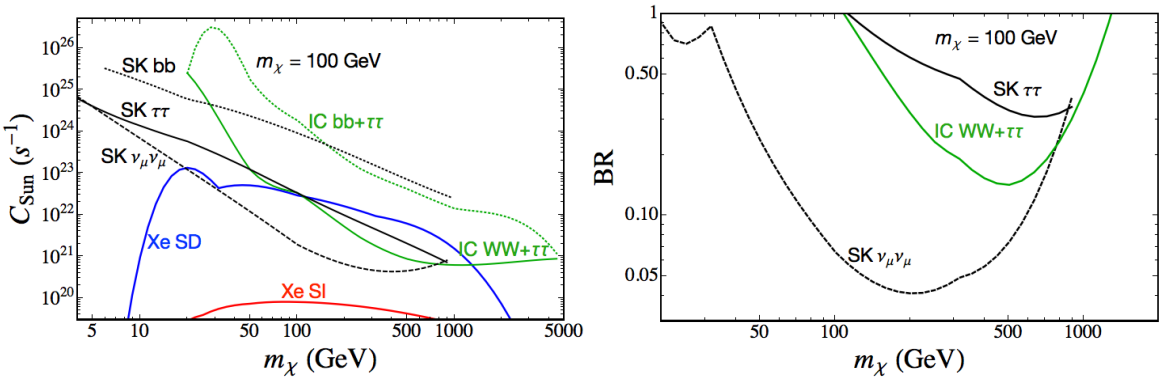

Figure 2. Left) Lower bounds on the DM capture rate in the Sun for xenon. Both SI (red curves) and SD (blue curves) interactions are shown. Right) Upper bounds on the annihilation channels using limits from the neutrino observatories IceCube (IC) [18] and Super-Kamiokande (SK) [19].

$$\geq 4\pi\mathcal{C}\sum_A A_{\rm eff}^2\int_0^{R_{\rm S}} dr r^2\rho_A(r)\int_{v_{\rm thr}}^{v_{\rm cross}^A} dv\,\tilde{f}(v)\,v\,\mathcal{F}_A(v,r)\,,$$

where from the first to the second line we changed the lower integration limit from zero to the threshold of the DD experiment, $v_{\rm thr}$. $\mathcal{F}_A$ is an integral over the nuclear form factors of the elements in the Sun, and ρ_A their density. This lower bound on the capture is independent of $f(v)$, $v_{\rm esc}$, σ_χ and ρ_χ. If equilibrium between capture and annihilations in the Sun is reached, as expected, the annihilation rate is completely determined in terms of the capture by $\Gamma_{\rm Sun} = C_{\rm Sun}/2$. Therefore, we can compare the lower bounds on $C_{\rm Sun}$ with limits on the neutrino flux from IceCube (IC) [18] and Super-Kamiokande (SK) [19] (see also for instance refs. [20, 21, 22, 23] for analyses combining both signals).

In figure 2 we illustrate this procedure using a Maxwell-Boltzmann velocity distribution (SHM) to generate mock data for a Xe experiment with $E_{\rm thr} = 3, 5$ keV. We use a DM mass of 100 GeV and cross sections motivated by current upper limits, $10^{-45}\,{\rm cm}^2$ (SI) and $2\cdot 10^{-40}\,{\rm cm}^2$ (SD), with equal couplings to protons and neutrons. We show conservative results assuming that annihilations proceed with a 100% branching ratio into the channels $bb + \tau\tau$, $WW + \tau\tau$ and $\nu_\mu\nu_\mu$. We can see that Xe bounds are strongest for SD in the range $20 \lesssim m_\chi \lesssim 1000$ GeV, and weak for SI (being stronger for $m_\chi \gtrsim 50$ GeV). Non-trivial limits can be obtained for SD interactions and direct annihilations into neutrinos, $\tau\tau$ and WW.

3. Inelastic scattering (exothermic and endothermic) in DD and in the Sun

We have also extended this framework to the case of inelastic scattering, in which a DM particle of mass m_χ scatters into a high (low) mass state of mass $m_\chi + \delta$, with $\delta > 0$ (< 0). The capture rates are shown in fig. 3 for $\sigma = 10^{-42}$ cm^2, see also refs. [24, 25, 26]. Once current upper limits from DD are taken into account, captures are larger in the exothermic case, in particular in the SD case, while they are lower in the case of endothermic scattering.

A DD signal for inelastic scatterings would look rather different to the usual elastic case due to the different energy dependence of $v_{\rm m}(E_R)$, see left plot of fig. 4, with a maximum at some energy E_R. By extracting the halo integral $\eta(E_R)$, one can check if it is compatible with the signal being due to DM, as different energy branches contribute to the same velocity range and therefore should give the same rate, see ref. [12] for this *shape test*. From this observed $\eta(E_R)$ spectrum we can derive the minimum energy $E_{\rm min}^{\rm obs}$ where $\tilde{\eta}(E_{\rm R})$ is maximal (lowest $v_{\rm m}(E_R)$),

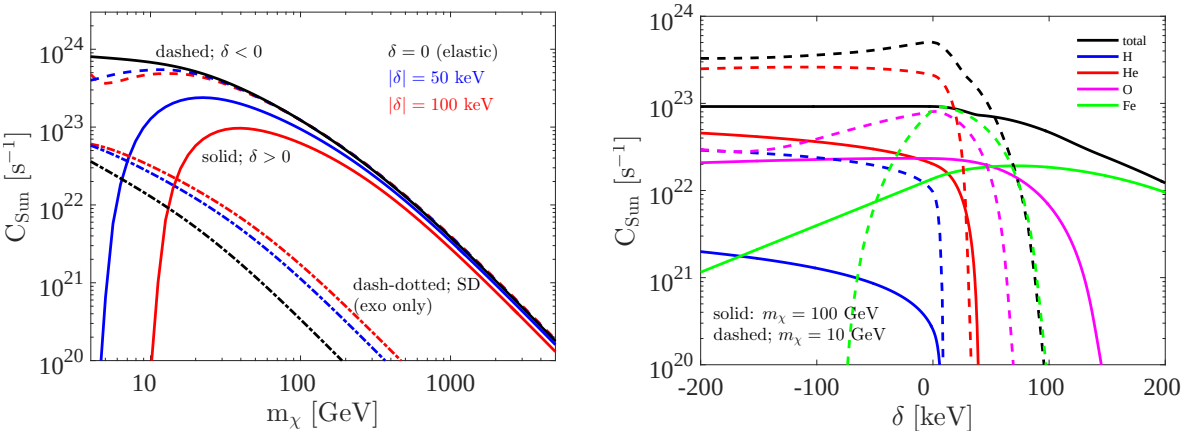

Figure 3. Left) Capture rate as a function of mass for $\delta = 50$ keV (blue) and $\delta = 100$ keV (red) for $\sigma = 10^{-42}$ cm^2. We show as solid lines the endothermic case and in dashed (dash-dotted) the SI (SD) exothermic cases. Right) Capture rates of different solar elements in terms of δ for $m_\chi = 10\,(100)$ GeV as dashed (solid) lines.

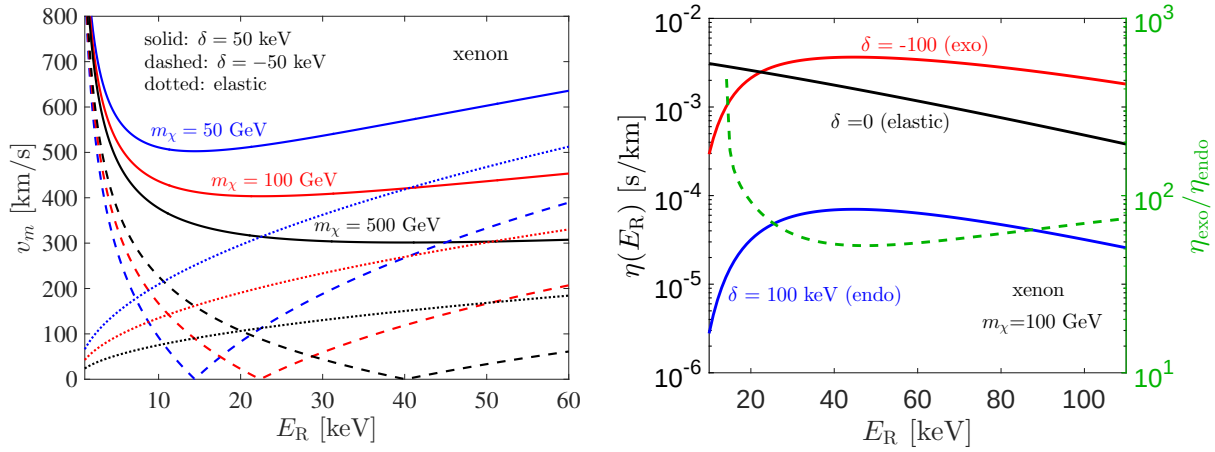

Figure 4. Left) We show v_m versus the recoil energy for xenon in the case of endothermic (solid) and exothermic (dashed) interactions with $\delta = 50\,(-50)$ keV, respectively. We show results for $m_\chi = 50, 100, 500$ GeV in blue, red and black respectively (from top to bottom). Right) $\eta(E_R)$ versus recoil energy for inelastic ($|\delta| = 100$ keV) endothermic and exothermic, and for elastic interactions, using $m_\chi = 100$ GeV. The ratio η_{exo}/η_{endo} is shown in green dashed.

and thus one can obtain the absolute value of the splitting δ as a function of m_χ (from eq. (2)):

$$|\delta\,(m_\chi)| = \frac{m_A}{\mu} E_{min}^{obs}\,. \tag{4}$$

3.1. Observing two inelastic direct detection signals

If two DD signals compatible with inelastic scattering are observed, i.e., they satisfy the *shape test* [12], from the maxima of the two halo integrals one can obtain the DM mass and the absolute value of the splitting via eq. 4:

$$m_\chi = \frac{m_1 E_1^{obs} - m_2 E_2^{obs}}{E_2^{obs} - E_1^{obs}}, \qquad |\delta| = \frac{E_1^{obs} E_2^{obs}(m_1 - m_2)}{m_1 E_1^{obs} - m_2 E_2^{obs}}\,. \tag{5}$$

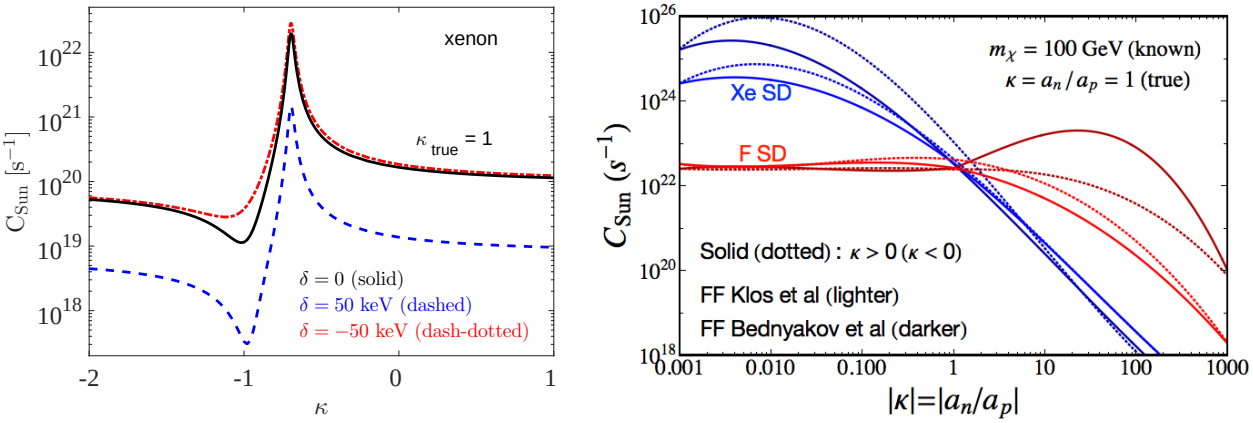

Figure 5. Left) The lower bounds on the capture rate as a function of $\kappa = f_n/f_p$. We use $\kappa_{\rm true} = 1$, $m_\chi = 100$ GeV, a SI cross section of 10^{-45} cm^2 and $|\delta| = 50$ keV. We also show the elastic case. Right) Lower bound for SD interactions for fluorine (proton dominated) and xenon (neutron dominated), see ref. [1] for details.

With the mass and the absolute value of the splitting, one can change from energy space to velocity space [6, 7] and compare the η of both experiments in the same velocity range using eq. (2) for the two possible signs of the splittings ($\delta > 0$ for endothermic, $\delta < 0$ for exothermic). By performing a likelihood fit to both cases, one can test whether it is the endothermic or the exothermic option the correct one to explain both signals. Moreover, the ratio of the signals will provide the couplings to neutrons and protons. With this information, one has a precise prediction for the capture rate in the Sun, see ref. [2] for some examples.

4. Isospin violation

Up to now we have assumed that one can extract the velocity distribution from the DD spectrum exactly, for which one needs to know the form factors (FF) and the couplings to neutrons/and protons ($\kappa \equiv a_n/a_p$). Uncertainties in these quantities will be transmitted to the bound on capture rate. In this case, the extracted velocity distribution for SI interactions will be:

$$\mathcal{C}\tilde{f}_{\rm extr}(v) = \mathcal{C}\tilde{f}(v)\frac{A^2_{\rm true}\,F^2_{\rm true}(E_R)}{A^2_{\rm wrong}\,F^2_{\rm wrong}(E_R)} - \frac{\tilde{\eta}(v)}{v}\frac{A^2_{\rm true}}{A^2_{\rm wrong}}\frac{d}{dv}\left(\frac{F^2_{\rm true}(E_R)}{F^2_{\rm wrong}(E_R)}\right), \qquad (6)$$

while for SD the A^2 factor is absent and the form factors encode the dependence on the couplings to protons/neutrons.

The implications for the lower bound on the capture are shown in fig. 5. One can see in the left plot (where we assumed a perfect knowledge of the SI FF) that if a DD signal in xenon is fitted with $\kappa \sim -0.7$, the large destructive interference implies that the cross section and thus the capture rate are large. The dip at $\kappa \sim -1$ is due to the destructive interference for the solar nuclei. On the right plot we show how the prediction varies depending on the spin of the element of the DD signal (dominated by the neutrons for xenon, by the protons for fluorine). This is due to the fact that the Sun is dominated by the protons, as thus depending on the element providing the DD signal both rates can largely decouple from each other (in the case of xenon), or become independent of the coupling to the protons (when the coupling to protons is larger than to the neutrons) in the case of fluorine, see ref. [1] for more details.

[1] Blennow M, Herrero-Garcia J and Schwetz T 2015 *JCAP* **1505** 036 (*Preprint* 1502.03342)
[2] Blennow M, Clementz S and Herrero-Garcia J 2015 (*Preprint* 1512.03317)
[3] Goodman M W and Witten E 1985 *Phys. Rev.* **D31** 3059
[4] Tucker-Smith D and Weiner N 2001 *Phys. Rev.* **D64** 043502 (*Preprint* hep-ph/0101138)
[5] Graham P W, Harnik R, Rajendran S and Saraswat P 2010 *Phys. Rev.* **D82** 063512 (*Preprint* 1004.0937)
[6] Fox P J, Kribs G D and Tait T M P 2011 *Phys. Rev.* **D83** 034007 (*Preprint* 1011.1910)
[7] Fox P J, Liu J and Weiner N 2011 *Phys. Rev.* **D83** 103514 (*Preprint* 1011.1915)
[8] Drukier A K, Freese K and Spergel D N 1986 *Phys. Rev.* **D33** 3495–3508
[9] Freese K, Frieman J A and Gould A 1988 *Phys. Rev.* **D37** 3388–3405
[10] Herrero-Garcia J, Schwetz T and Zupan J 2012 *JCAP* **1203** 005 (*Preprint* 1112.1627)
[11] Herrero-Garcia J, Schwetz T and Zupan J 2012 *Phys. Rev. Lett.* **109** 141301 (*Preprint* 1205.0134)
[12] Bozorgnia N, Herrero-Garcia J, Schwetz T and Zupan J 2013 *JCAP* **1307** 049 (*Preprint* 1305.3575)
[13] Blennow M, Herrero-Garcia J, Schwetz T and Vogl S 2015 *JCAP* **1508** 039 (*Preprint* 1505.05710)
[14] Herrero-Garcia J 2015 *JCAP* **1509** 012 (*Preprint* 1506.03503)
[15] Press W H and Spergel D N 1985 *Astrophys. J.* **296** 679–684
[16] Griest K and Seckel D 1987 *Nucl. Phys.* **B283** 681 [Erratum: Nucl. Phys.B296,1034(1988)]
[17] Gould A 1987 *Astrophys. J.* **321** 560
[18] Aartsen M G *et al.* (IceCube) 2013 *Phys. Rev. Lett.* **110** 131302 (*Preprint* 1212.4097)
[19] Tanaka T *et al.* (Super-Kamiokande) 2011 *Astrophys. J.* **742** 78 (*Preprint* 1108.3384)
[20] Ferrer F, Ibarra A and Wild S 2015 *JCAP* **1509** 052 (*Preprint* 1506.03386)
[21] Serpico P D and Bertone G 2010 *Phys. Rev.* **D82** 063505 (*Preprint* 1006.3268)
[22] Arina C, Bertone G and Silverwood H 2013 *Phys. Rev.* **D88** 013002 (*Preprint* 1304.5119)
[23] Kavanagh B J, Fornasa M and Green A M 2015 *Phys. Rev.* **D91** 103533 (*Preprint* 1410.8051)
[24] Nussinov S, Wang L T and Yavin I 2009 *JCAP* **0908** 037 (*Preprint* 0905.1333)
[25] Menon A, Morris R, Pierce A and Weiner N 2010 *Phys. Rev.* **D82** 015011 (*Preprint* 0905.1847)
[26] Shu J, Yin P f and Zhu S h 2010 *Phys. Rev.* **D81** 123519 (*Preprint* 1001.1076)